Supporting Information for

Reductive Hexachloroethane Degradation by $S_2O_8^{\bullet-}$ with Thermal Activation of Persulfate under Anaerobic Conditions

Changyin Zhu[a,b], Fengxiao Zhu[a], Cun Liu[a], Ning Chen[a,b], Dongmei Zhou[a], Guodong Fang [a,*], Juan Gao[a,*]

[a] *Key Laboratory of Soil Environment and Pollution Remediation, Institute of Soil Science, Chinese Academy of Sciences, Nanjing 210008, PR China*

[b] *University of Chinese Academy of Sciences, Beijing 100049, PR China*

[*]*Corresponding author.*

E-mail address: gdfang@issas.ac.cn (G.D. Fang)

juangao@issas.ac.cn (J. Gao).

27 pages
5 text
18 figures

Contents

Text S1: Chemicals.

HCA was purchased from Dr. Ehrenstorfer GmbH (99%, Augsburg, Germany), 5,5-Dimethyl-1-pyrrolidine N-oxide (DMPO, 97%) were obtained from Sigma–Aldrich (Saint Louis, MO, USA). Sodium persulfate, phenol, *tert*-butyl alcohol (TBA), carbon tetrachloride, potassium dichromate, potassium iodide, sodium chloride, sodium nitrate, sodium carbonate, sodium bicarbonate and sodium hydroxide were obtained from Chinese National Medicines Corporation Ltd. (Shanghai, China). All of the chemicals were of analytical grade. Deionized water with a resistivity of 18 MΩ•cm^{-1} was used for preparing aqueous solutions.

Text S2: Experimental procedures for the degradation of HCA and DDT in soil

HCA-spiked soil samples were prepared as follows: Clean soil was collected from Nanjing, Jiangsu Province (31 °95' N, 118 °83' E). The soil was dried indoors and ground to pass through a 0.3 mm sieve. The soil had a pH of 6.8 and an organic content of 1.0 wt%. The concentration of HCA was 236 mg kg^{-1}. 200 g uncontaminated soil was placed in a 500-mL beaker and spiked with 2 mM HCA stock solution 100 mL. The soil was then stirred vigorously for 15 min with a glass rod to promote homogeneous distribution of HCA. And then the spiked soil was placed in a fume hood to eliminate the solvents. To make sure that the entire quantity of n-hexane solvent had been eliminated, the weight of the mixture was monitored at intervals until it remained unchanged.

Soil polluted with DDT from an insecticide factory in Suzhou, Jiangsu Province (31 °32' N, 120 °62' E), was sampled at a depth of 0.2 m. The soil was dried indoors

and ground to pass through a 0.3 mm sieve. The soil had a pH of 6.7 and an organic content of 1.0 wt%. The main pollutant detected in the soil was *o,p′*-DDT at a concentration of 179 mg kg^{-1}.

We investigated the remediation of HCA or DDT contaminated soil by thermal activation of PS under anaerobic conditions. All experiments were conducted in 9.0 mL brown serum bottles containing 4.0 mL or 5.0 mL of reaction suspension for HCA or DDT degradation, respectively. First, 0.5 g of polluted soil transferred to the bottles and dispersed with deionized water. PS solution was added to each bottle to a final concentration of 10 mM or 50 mM for HCA or DDT degradation, respectively. The bottles were placed on a reciprocating shaker at a speed of 200 rpm and a temperature of 50 ℃. At specified time intervals, the bottles were taken out and cooled to 0 ℃ by putting them immediately in ice water to quench the reactions. A control experiment under aerobic conditions was also performed. All experiments were performed in triplicate. After the reaction, the reaction suspension was allowed to stand. HCA: 2.0 mL of hexane added into the serum bottles. The mixture was shaken for 1.0 h to extract HCA and then subjected to gas chromatography (GC) analysis. DDT: The supernatant was then discarded and the soil was freeze-dried, and then 6.0 mL of hexane/acetone solution (1:1, v/v) was added to the vials. The vials were then agitated on a reciprocating shaker (200 rpm) for 1.0 h to extract DDT for GC analysis.

Text S3: Analytical methods

HCA, DDT and HCA products concentrations during the reaction were analyzed with a gas chromatograph (Aglient7820, Palo Alto, USA) equipped with Ni^{63} electron

capture detection. Chromatographic separation was accomplished with a 30 m × 0.32 mm × 0.25 μm HP-5 column (J&W Scientific Inc., Folsom, USA). We used nitrogen as the carrier gas (flow rate of 1.0 mL min^{-1}) and a sample injection volume of 1.0 μL. For HCA analysis, the temperatures for the injector and the detector were 250 and 300 ℃, respectively. The initial temperature of the oven was 80 ℃ (kept for 1.0 min), and then the temperature was increased to 140 ℃ at a rate of 10 ℃ min^{-1}. For DDT analysis, the temperatures for the injector and detector were 215 and 300 ℃, respectively. The initial temperature of the oven was 60 ℃, which held 1.0 min. The temperature was then increased to 190 ℃ at a rate of 30 ℃ min^{-1} and held there for 1.0 min. Subsequently, the temperature was increased to 250 ℃ at a rate of 5 ℃ min^{-1} and held there for 2.0 min. For C_2Cl_4, HC_2Cl_5 and $HCCl_3$ analysis, the temperatures for the injector and the detector were 250 and 300 ℃, respectively. The initial temperature of the oven was 40 ℃ (kept for 3.0 min), and then the temperature was increased to 140 ℃ at a rate of 10 ℃ min^{-1}. The degradation products of HCA were analyzed by a gas chromatograph-mass spectrometer (GC–MS, Varian CP 3800 Saturn 2200, Palo Alto, USA) after headspace injection. Chromatographic separation was accomplished with a 30 m × 0.25 mm × 0.25 μm CP-5 column. Helium at a flow rate of 1.0 mL min^{-1} was used as the carrier gas. The sample injection volume was 500 μL, and the initial temperature for the injector was 200 ℃. The initial temperature of the oven was 50 ℃ for 2.0 min. The temperature was increased to 140 ℃ at a rate of 5 ℃ min^{-1} and held there for 3.0 min. Subsequently, the temperature was increased to 250 ℃ at a rate of 10 ℃ min^{-1} and

held there for 5.0 min.

PS concentrations were determined with the spectrophotometric method using a UV–visible spectrophotometer (UV2700, Shimadzu, Kyoto, Japan),[1] and the concentrations of chloride generated were analyzed by ion chromatography (ICS 1100, Dionex, Sunnyvale, USA). Total organic carbon (TOC) was measured using a TOC analyzer (Analytik Jena AG, multi N/C 3100, Germany).

EPR studies: Experiments of thermally activated PS were conducted in a mixed solution of PS (10 mM-1M), and 0.1 M spin trapping agent DMPO solution, and placed in oven with temperature of 50-60 ^{o}C. $FeSO_4$ or $Fe(NO_3)_3$ was added into the mixture in the experiment of PS activation by Fe(II)/Fe(III) with temperature of 20 ^{o}C. The electron paramagnetic resonance (EPR) spectra were obtained using a Bruker EMX/plus spectrometer (Karlsruhe, Germany), The conditions were: resonance frequency of 9.85 GHz, microwave power of 20.0 mW, modulation frequency of 100 kHz, modulation amplitude of 1.0 G, sweep width of 200 G, time constant of 40.96 ms, sweep time of 81.92 s, and receiver gain of 1.0×10^3. In the sample vials, 100 mM 5,5-dimethyl -1-pyrroline-N-oxide (DMPO) was added as the spin-trap agent.

The dissolved O_2 in the solution was analyzed by dissolved oxygen meter (Seven2Go Pro S9, Zurich, Swiss), A pH/Ion meter (Thermo Orion 5 star, Massachusetts, USA) equipped with a pH electrode (Thermo 911600) was used to monitor solution pH.

Text S4: The second reaction rate constant of $S_2O_8^{\bullet-}$ with HCA. The difficulty in measuring $S_2O_8^{\bullet-}$ concentration caused it impossible to directly calculate the second

reaction rate constant between $S_2O_8^{\bullet-}$ and HCA in the present study. After carefully checking the literatures, the second reaction rate constant was estimated to be analogous to the second reaction rate constant between methanol (MeOH) radical and HCA, since MeOH radical has similar properties to $S_2O_8^{\bullet-}$ radical interacting with HCA via reductive degradation pathways.[2] Additional experiments were conducted to compare the reactivities of HCA with MeOH radical and $S_2O_8^{\bullet-}$ radical in the PS/heat system under anaerobic conditions. As shown in Figure S10, methanol has limited effects on HCA degradation with its concentration increased from 0.4 to 250 mM. MeOH radical concentration was estimated to be higher than that of $S_2O_8^{\bullet-}$ radical at higher concentration (e.g., [MeOH] > 10 mM) according to equation 1 and 2:

$$SO_4^{\bullet-} + S_2O_8^{2-} \rightarrow S_2O_8^{\bullet-} + SO_4^{2-} \qquad k=6.3\times10^5\ M^{-1}s^{-1} \qquad (1)$$

$$SO_4^{\bullet-} + CH_3OH \rightarrow {}^{\bullet}CH_2OH + SO_4^{2-} + H^+ \quad k=3.2\times10^6\ M^{-1}S^{-1} \qquad (2)$$

Since the second reaction rate constant between MeOH radical and HCA fell in the range of $1\times10^6 \sim 3\times10^7$ M^{-1} s^{-1}, it was therefore estimated that $S_2O_8^{\bullet-}$ has a comparable reactivity to if not higher than MeOH radical and its second reaction rate constants was roughly at an order of about 10^6-10^7 $M^{-1}s^{-1}$.

Furthermore, the reaction rate constant was also evaluated on the basis of steady-concentrations of sulfate radical and $S_2O_8^{\bullet-}$. Briefly, our previous study reported that sulfate radical was dominant free radical during persulfate thermal activation under acidic conditions and its concentration was about 10^{-13} M.[3] In the PS/heat system in the absence of oxygen, $S_2O_8^{\bullet-}$ was formed and sulfate radical also regenerated via reactions (1, 3).

$$S_2O_8^{\bullet-}+S_2O_8^{2-}+2H_2O\rightarrow SO_4^{2-}+SO_4^{\bullet-}+2HSO_5^{-}+2H^{+} \quad (3)$$

Conseqeuently, it was hypothezied that the steady-concentration of $S_2O_8^{\bullet-}$ was up to 10^{-13} M if sulfate radical was completely converted to $S_2O_8^{\bullet-}$. According to the apparent rate constant of HCA degraded by $S_2O_8^{\bullet-}$ (2.2×10^{-3} μM min^{-1}), the second reaction rate constant (k) would be $\geqslant$ 3.3×10^{6} $M^{-1}s^{-1}$, which was consistent with the value obtained from the MeOH competition experiment. It is altogether suggested that the reaction rate of $S_2O_8^{\bullet-}$ and HCA falls in the range of typical reactions between radicals and organics and the reaction is the rate-limiting step in HCA degradation.

Text S5: Computational Methods. Density functional theory (DFT) calculations were conducted to evaluate the initial reaction pathways of DMPO-S_2O_8 adduct decomposition and $S_2O_8^{\bullet-}$ radical interacting with HCA, respectively. The possible structures and energetics of reaction intermediates and products associated with the proposed reaction pathways were determined using the Gaussian16 software package.[4] Solvent effects were included by using continuum solvation model (SMD).[5] Full geometry optimizations of all species were performed using the Long range-corrected CAM-B3LYP with 6-31++G(d,p) basis set.[4] The Gibbs free energy for all structures was calculated using the standard equations of statistical mechanics. The optimized structures and energetics of DMPO-S_2O_8 decomposition are shown in Figure S5, while the theoretical reaction pathways of $S_2O_8^{\bullet-}$ radical interacting with HCA are shown in Figure S11.

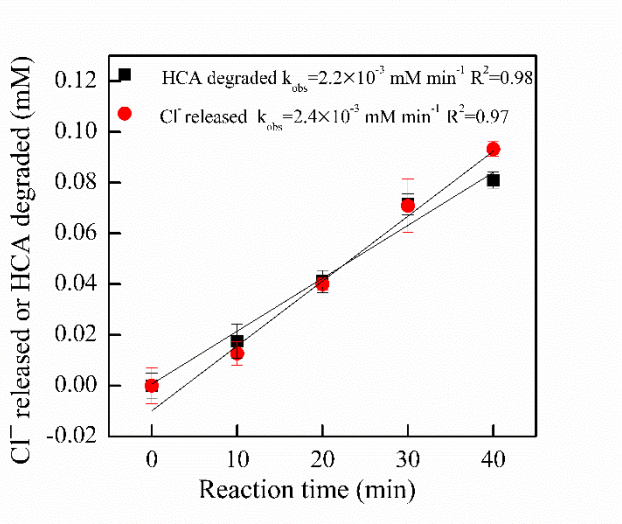

Figure S1 Plot of k_{obs} of chloride release versus the amount of HCA degraded. Reaction conditions: [PS] = 10 mM, [HCA] = 100 μM, 50 °C, initial pH of 4.2, reaction for 60 min.

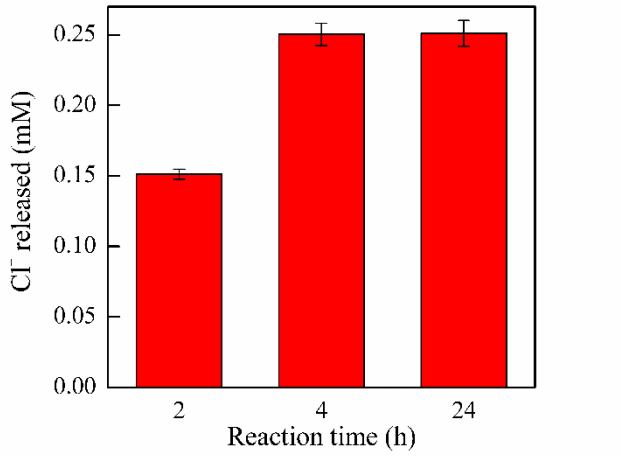

Figure S2 Amount of chloride released when the time was prolonged to 24 h in the absence of oxygen with thermally activated PS. Reaction conditions: [PS] = 10 mM, [HCA] = 100 μM, 50 °C, initial pH of 4.2, reaction for 24 h.

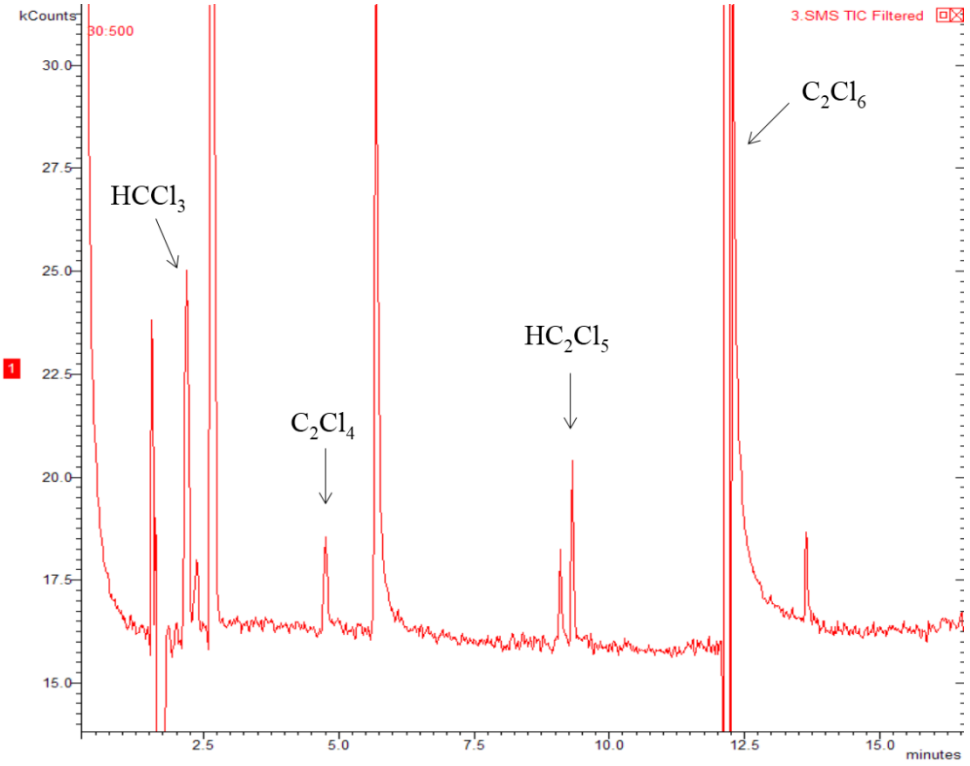

Figure S3 GC–MS spectrum of HCA degradation with thermally activated PS in the absence of oxygen. Reaction conditions: [PS] = 10 mM, [HCA] = 0.1 mM, 50 °C, initial pH of 4.2, reaction for 30 min.

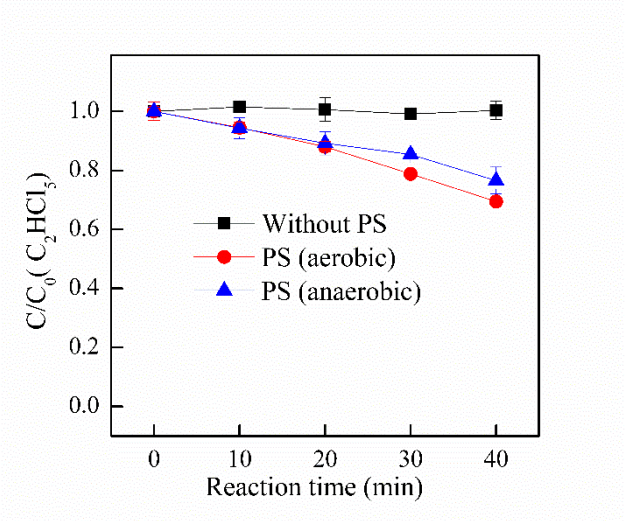

Figure S4 Degradation of HC_2Cl_5 with thermally activated PS in the absence of oxygen. Reaction conditions: [PS] = 10 mM, [HC_2Cl_5] = 0.1 mM, 50 °C, initial pH of 4.2, reaction for 40 min.

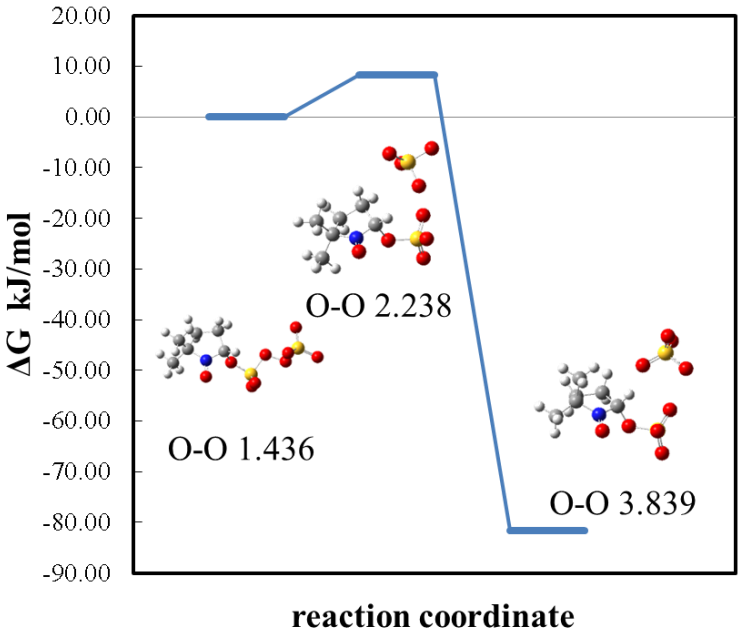

Figure S5 Gibbs free energy profiles for the initial step of DMPO-S_2O_8 decomposition via breakage of O-O bond as calculated by the DFT/SMD method at the CAM-B3LYP/6-31++G(d,p) level. The relative free energies shown include the zero-point and thermal corrections, and solvent effects. The optimized structure and O-O distance for each complex was depicted in the graph. Color scheme: carbon in grey, oxygen in red, sulfur in yellow, hydrogen in white.

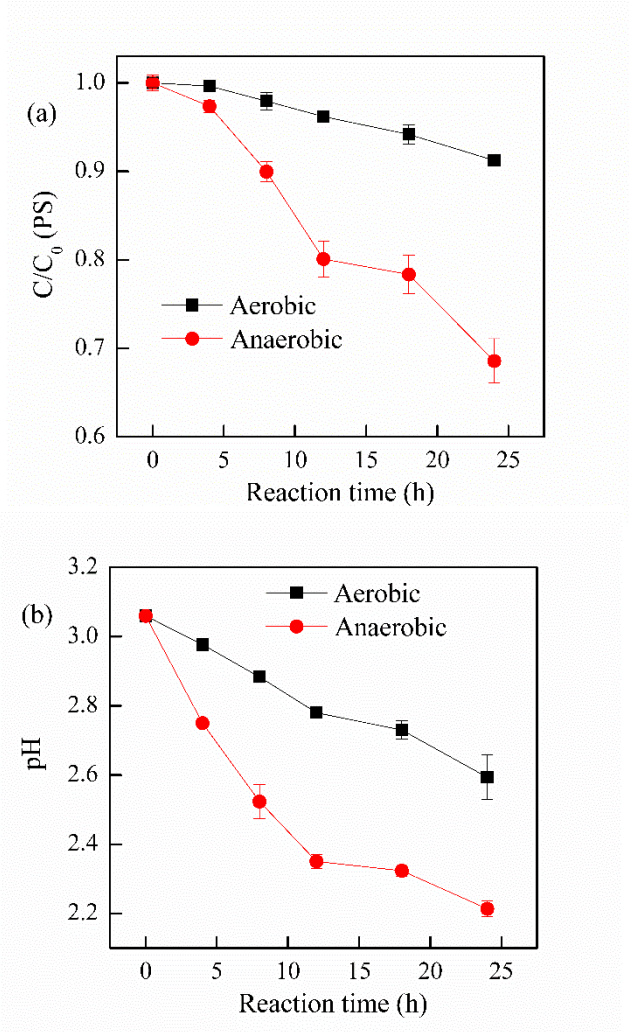

Figure S6 Effect of oxygen on (a) PS consumption and (b) solution pH change. Reaction conditions: [PS] = 10 mM, 50 °C, initial pH of 3.0, reaction for 24 h.

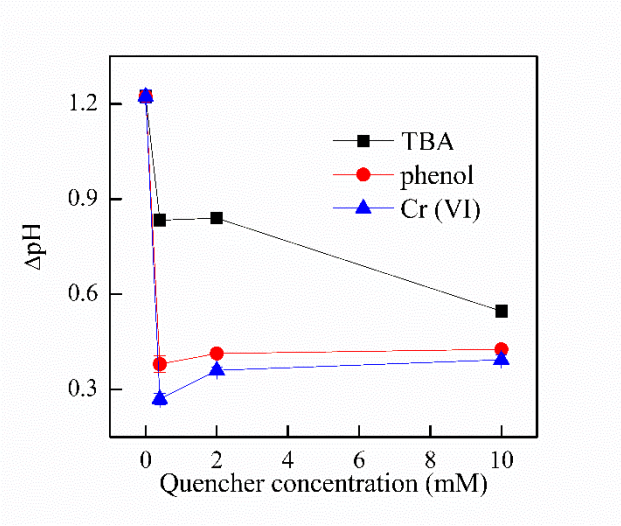

Figure S7 Effect of quencher on the variation of (a) solution pH and (b) H^+ production. Reaction conditions: [PS] = 10 mM, [HCA] = 1.0 μM, 50 °C, initial pH of 4.2, reaction for 60 min.

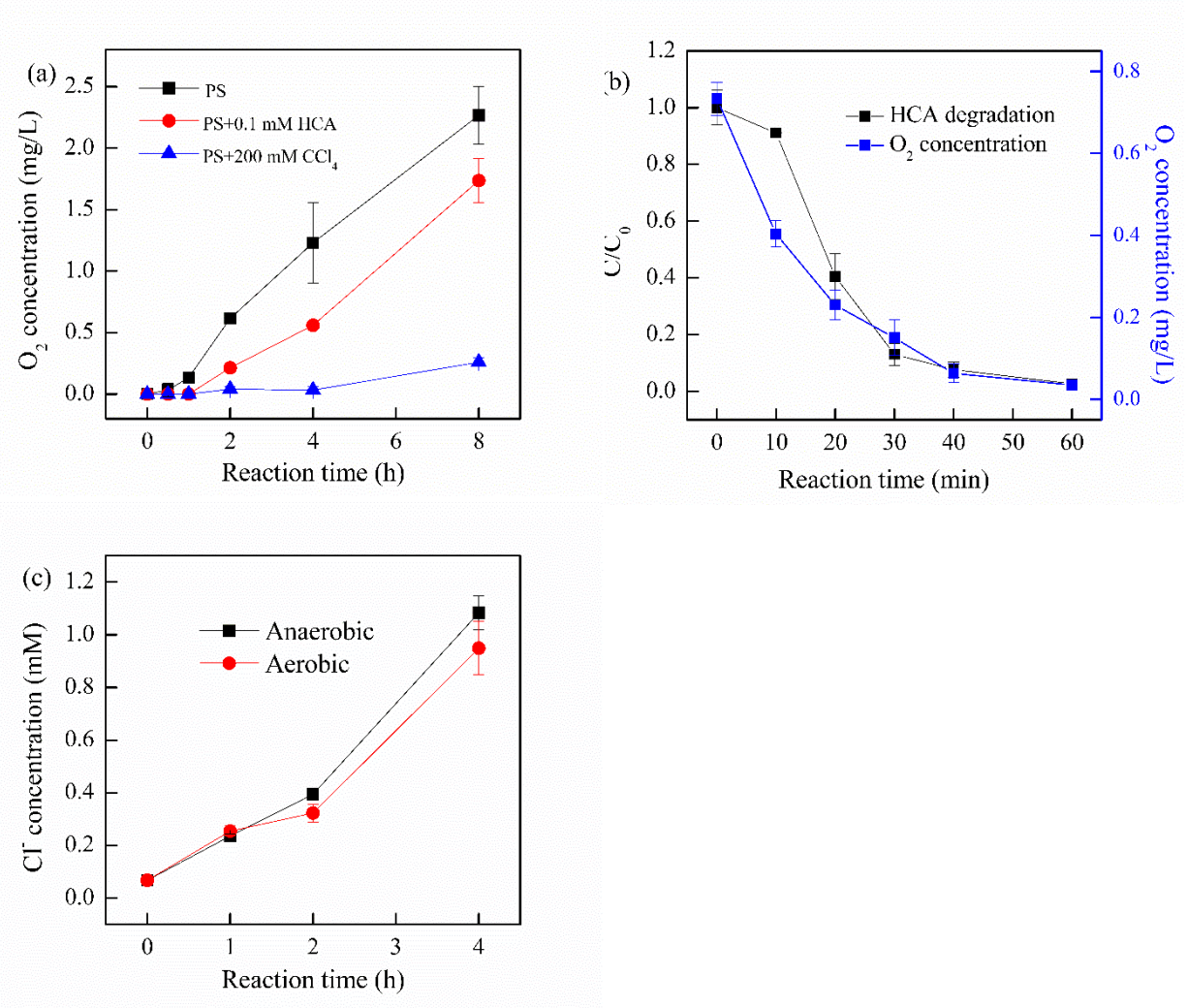

Figure S8 (a) DO concentration in thermally activated PS with contaminants, (b) the degradation of HCA and DO with initial DO concentration of 0.73 mg/L, (c) effect of oxygen on the degradation of CCl_4 in thermally activated PS. Reaction condition: [PS] = 10 mM, 50 ℃, initial pH of 4.2, (a) [HCA]=0.1 mM, [CCl_4] = 200 mM, reaction for 8 h, (b) [HCA]=1 μM, reaction for 60 min, (c) [CCl_4] = 200 mM, reaction for 4 h.

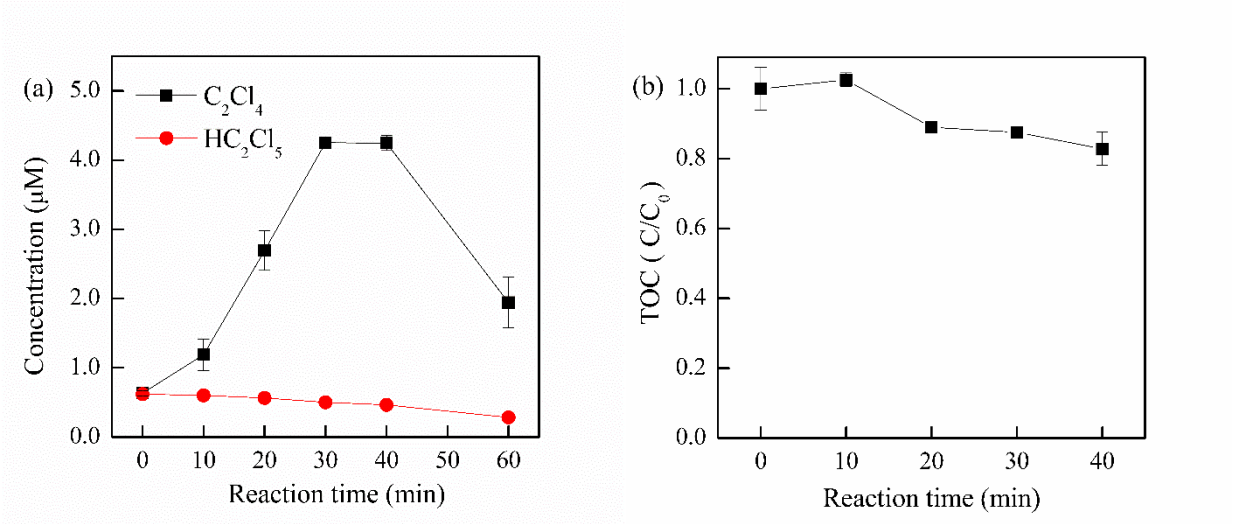

Figure S9 (a) Production of C_2Cl_4 and HC_2Cl_5 with thermally activated PS in the absence of oxygen, (c) the removal of TOC with thermally activated PS in the absence of oxygen. Reaction conditions: [PS] = 10 mM, 50 °C, initial pH of 4.2, reaction for 60 or 40 min, (a,c) [HCA] = 0.1 mM, (b) [HC_2Cl_5] = 0.1 mM.

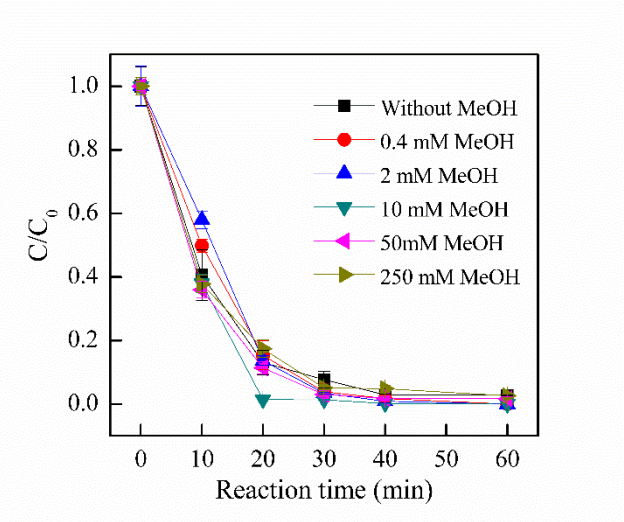

Figure S10 Effects of MeOH concentration on HCA degradation in the absence of oxygen. Reaction conditions: [HCA] = 1. 0 μM, [PS] = 10 mM, [MeOH] = 0, 0.4, 2, 10, 50, 250 mM, 50 ℃, initial pH of 4.2, reaction for 60 min.

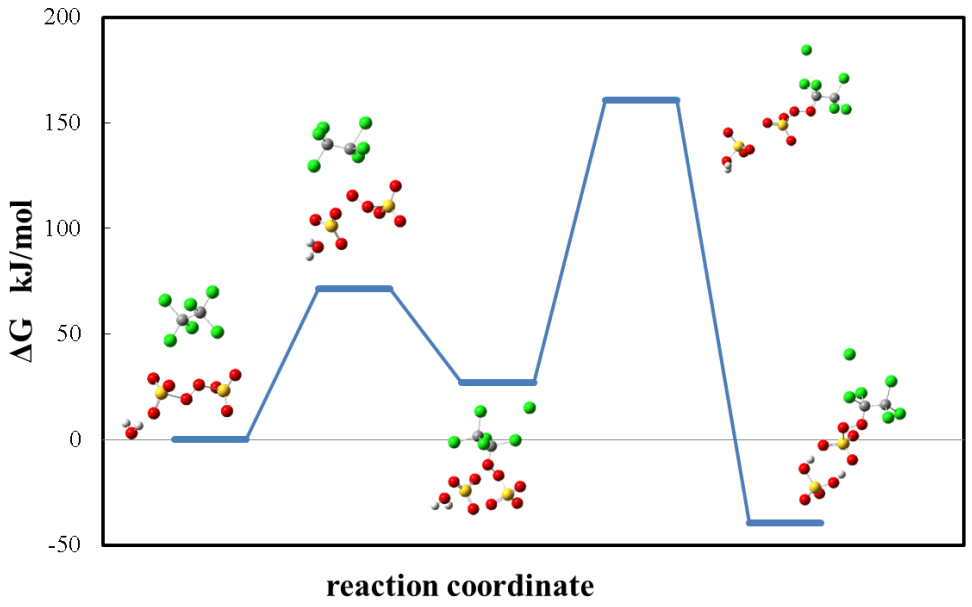

Figure S11 Gibbs free energy profiles for the initial steps of $S_2O_8^{\bullet-}$ radical interacting with HCA as calculated by the DFT/SMD method at the CAM-B3LYP/6-31++G(d,p) level. The relative free energies shown include the zero-point and thermal corrections, and solvent effects. The optimized structure for each complex was depicted in the graph. Color scheme: Carbon in grey, Oxygen in red, sulfur in yellow, Hydrogen in white.

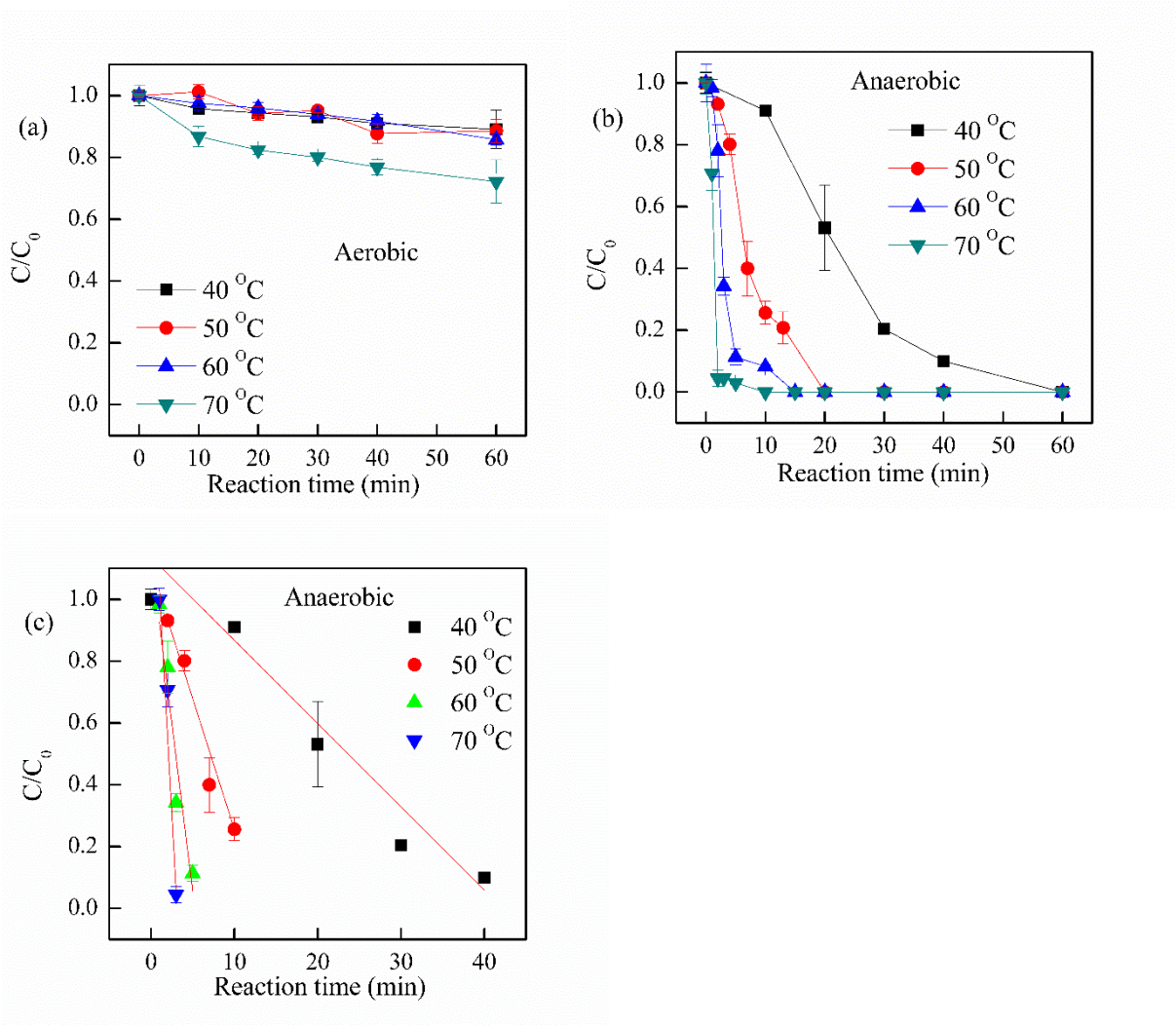

Figure S12 Effects of temperature on HCA degradation in the (a) presence or (b) absence of oxygen, (c) kinetic fitting of HCA degradation with varies temperature. Reaction conditions: [HCA] = 1.0 μM, [PS] = 10 mM, temperatures of 40, 50, 60, and 70 °C, initial pH of 4.2, reaction for 60 min.

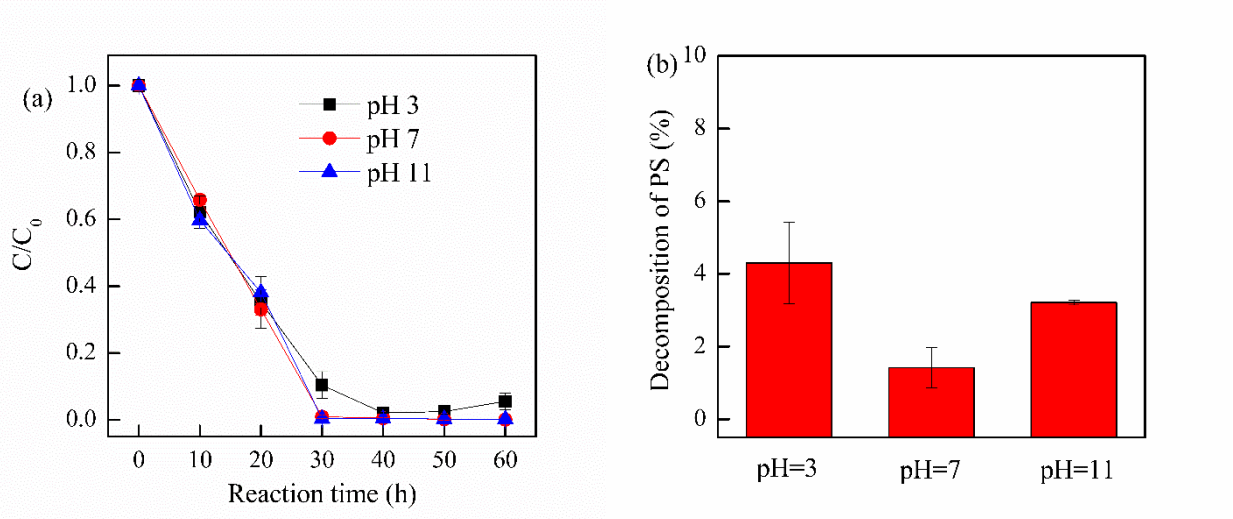

Figure S13 Effects of solution pH on (a) HCA degradation for 60 min and (b) PS decomposition for 30 min in the absence of oxygen. Reaction conditions: [PS] = 10 mM, [HCA] = 1.0 mM, initial pH of 4.2, 50 °C.

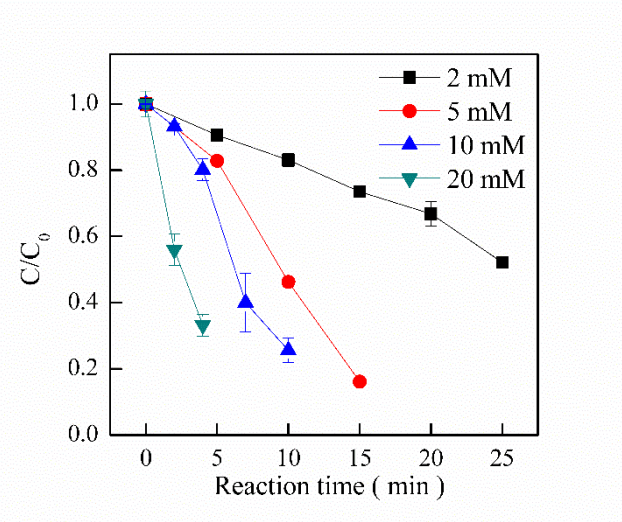

Figure S14 Effects of PS concentration on HCA degradation in the absence of oxygen. Reaction conditions: [PS] = 2, 5, 10, 20 mM, [HCA] = 1. 0 μM, 50 °C, initial pH of 4.2, reaction for 4-25 min.

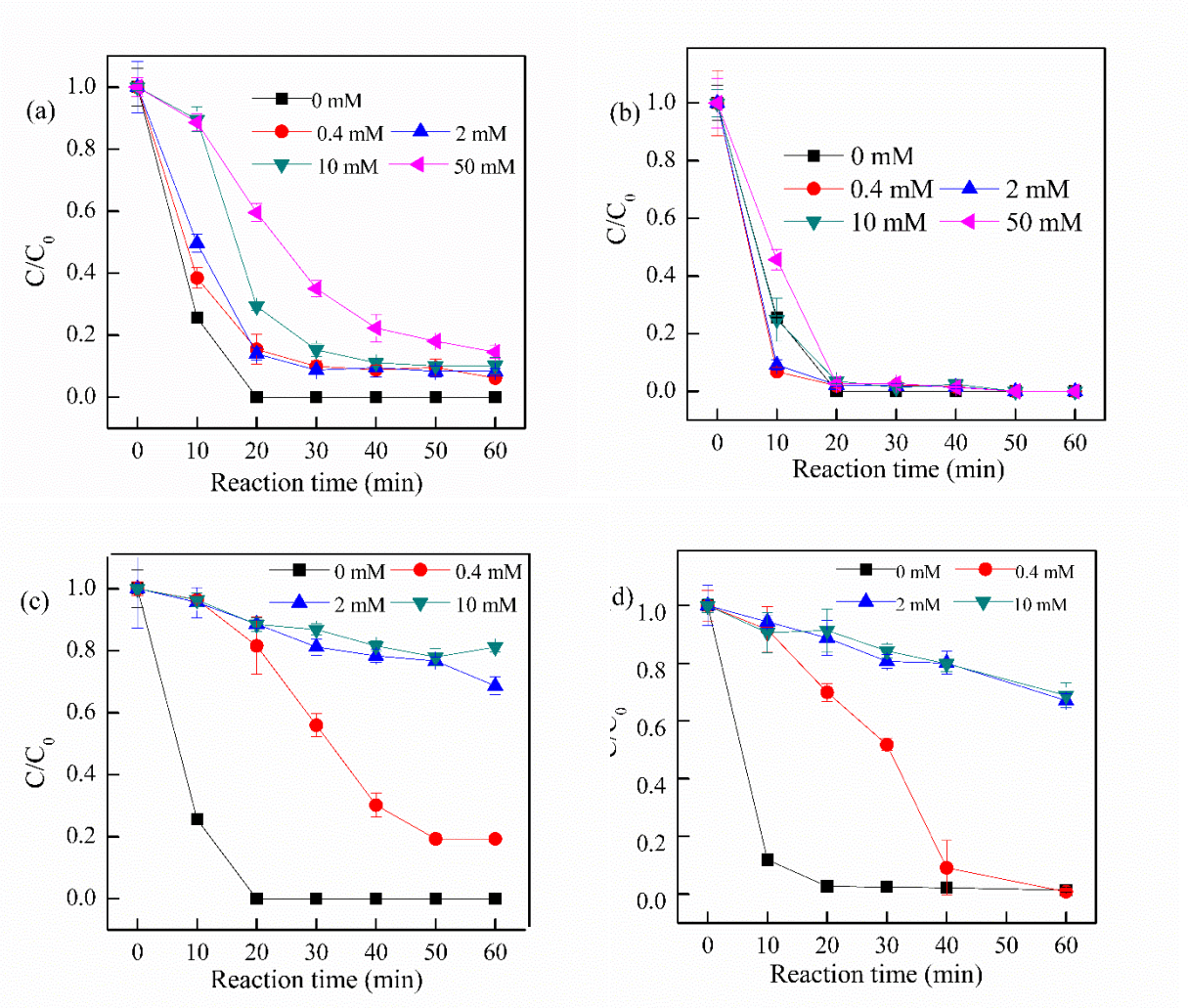

Figure S15 Effects of Cl^-, NO_3^-, CO_3^{2-} and HCO_3^- on the HCA degradation in the absence of oxygen. Reaction conditions: [PS] = 10 mM, [HCA] = 1.0 μM, 50 °C, reaction for 60 min, (a,b) [Cl^-, NO_3^-] = 0, 0.4, 2.0, 10, 50 mM, initial pH of 4.2, (c,d) [CO_3^{2-}, HCO_3^-] = 0, 0.4, 2.0, 10 mM, initial pH of 9.9, 10.5 and 10.9 for 0.2, 2 and 10 mM CO_3^{2-}, respectively, and was 6.8, 8.5 and 9.0 for 0.2, 2 and 10 mM HCO_3^-, respectively.

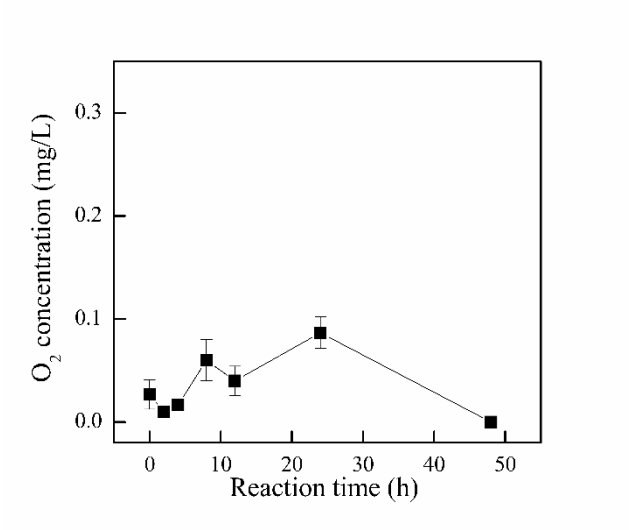

Figure S16 The DO concentration of HCA degradation in soil with thermally activated PS in absence of oxygen. Reaction conditions: [PS] = 10 mM, [HCA] = 236 mg kg^{-1}, 50 ℃, reaction for 72 h.

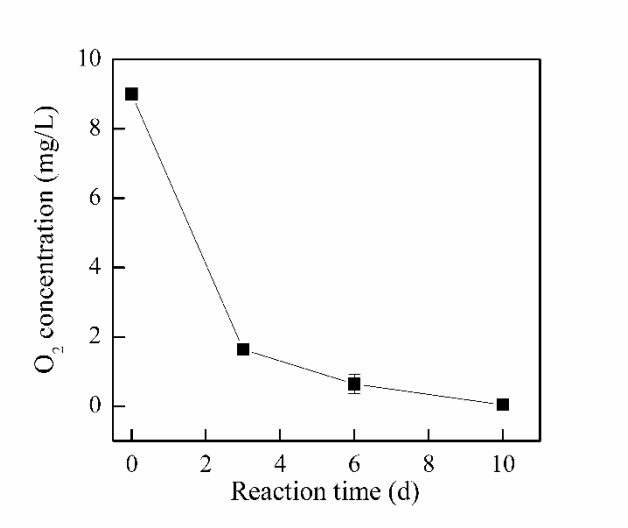

Figure S17 DO concentration in soil and water mixture. Reaction condition: 4.0 g soil with full of water in 9.0 mL brown serum at temperature of 20 ^{o}C.

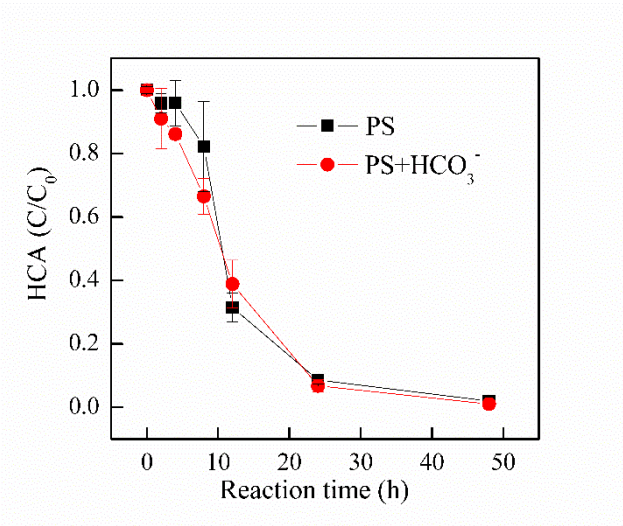

Figure S18 Effects of HCO_3^- on HCA degradation in soil in the absence of oxygen. Reaction conditions: [PS] = 10 mM, [HCO_3^-]=10 mM, [HCA] = 236 mg kg^{-1}, 50 °C, reaction for 48 h.

References

(1) Liang, C.; Huang, C. F.; Mohanty, N.; Kurakalva, R. M. A rapid spectrophotometric determination of persulfate anion in ISCO. *Chemosphere* **2008**, *73*, 1540-1543.

(2) Gonzalez, M. C; Le Roux, G. C.; Rosso, J. A.; Braun, A. M. Mineralization of CCl_4 by the UVC-photolysis of hydrogen peroxide in the presence of methanol. *Chemosphere*, **2007**, 69(8): 1238-1244.

(3) Fang, G. D.; Dionysiou, D. D.; Zhou, D. M.; Wang, Y.; Zhu, X. D.; Fan, J. X.; Cang, L.; Wang, Y. J. Transformation of polychlorinated biphenyls by persulfate at ambient temperature. *Chemosphere*, **2013**, 90(5): 1573-1580.

(4) Gaussian 16, M. J. Frisch, G. W. Trucks, H. B. Schlegel, G. E. Scuseria, M. A. Robb, J. R. Cheeseman, G. Scalmani, V. Barone, G. A. Petersson, H. Nakatsuji, X. Li, M. Caricato, A. Marenich, J. Bloino, B. G. Janesko, R. Gomperts, B. Mennucci, H. P. Hratchian, J. V. Ortiz, A. F. Izmaylov, J. L. Sonnenberg, D. Williams-Young, F. Ding, F. Lipparini, F. Egidi, J. Goings, B. Peng, A. Petrone, T. Henderson, D. Ranasinghe, V. G. Zakrzewski, J. Gao, N. Rega, G. Zheng, W. Liang, M. Hada, M. Ehara, K. Toyota, R. Fukuda, J. Hasegawa, M. Ishida, T. Nakajima, Y. Honda, O. Kitao, H. Nakai, T. Vreven, K. Throssell, J. A. Montgomery, Jr., J. E. Peralta, F. Ogliaro, M. Bearpark, J. J. Heyd, E. Brothers, K. N. Kudin, V. N. Staroverov, T. Keith, R. Kobayashi, J. Normand, K. Raghavachari, A. Rendell, J. C. Burant, S. S. Iyengar, J. Tomasi, M. Cossi, J. M. Millam, M. Klene, C. Adamo, R. Cammi, J. W. Ochterski, R. L. Martin, K. Morokuma, O. Farkas, J. B. Foresman, and D. J. Fox, Gaussian, Inc., Wallingford CT, **2016**.

(5) A. V. Marenich, C. J. Cramer, and D. G. Truhlar, Universal solvation model based on solute electron density and a continuum model of the solvent defined by the bulk dielectric constant and atomic surface tensions, *J. Phys. Chem. B* **2009**, *113*, 6378-6396.

(6) T. Yanai, D. Tew, and N. Handy, A new hybrid exchange-correlation functional using the Coulomb-attenuating method (CAM-B3LYP), *Chem. Phys. Lett*. **2004**, *393*, 51-57.